This is a repository copy of *Influence of nickel-based catalysts on syngas production from carbon dioxide reforming of waste high density polyethylene*.

White Rose Research Online URL for this paper:
http://eprints.whiterose.ac.uk/89452/

Version: Accepted Version

**Article:**

Saad, JM, Nahil, MA, Wu, C et al. (1 more author) (2015) Influence of nickel-based catalysts on syngas production from carbon dioxide reforming of waste high density polyethylene. Fuel Processing Technology, 138. 156 - 163. ISSN 0378-3820

https://doi.org/10.1016/j.fuproc.2015.05.020

© 2015, Elsevier. Licensed under the Creative Commons Attribution-NonCommercial-NoDerivatives 4.0 International
http://creativecommons.org/licenses/by-nc-nd/4.0/

**Reuse**
Unless indicated otherwise, fulltext items are protected by copyright with all rights reserved. The copyright exception in section 29 of the Copyright, Designs and Patents Act 1988 allows the making of a single copy solely for the purpose of non-commercial research or private study within the limits of fair dealing. The publisher or other rights-holder may allow further reproduction and re-use of this version - refer to the White Rose Research Online record for this item. Where records identify the publisher as the copyright holder, users can verify any specific terms of use on the publisher's website.

**Takedown**
If you consider content in White Rose Research Online to be in breach of UK law, please notify us by emailing eprints@whiterose.ac.uk including the URL of the record and the reason for the withdrawal request.

eprints@whiterose.ac.uk
https://eprints.whiterose.ac.uk/

# Influence of nickel-based catalysts on syngas production from carbon dioxide reforming of waste high density polyethylene

Juniza Md Saad, Mohamad Anas Nahil, Chunfei Wu and Paul T. Williams*

Energy Research Institute
The University of Leeds, Leeds, LS2 9JT, UK
(*Tel:  #44 1133432504; Email: p.t.williams@leeds.ac.uk)

## Abstract:

Syngas production ($H_2$ and CO) from carbon dioxide reforming of high density polyethylene (HDPE) over Ni-Al catalyst was evaluated in a two-stage fixed bed reactor. Syngas production was favoured by $CO_2$ addition, with the highest production of 138.81 $\text{mmol}_{\text{syngas}}\ \text{g}^{-1}_{\text{HDPE}}$, which was about six times higher than non-catalytic, non-$CO_2$ addition. The catalytic performances of nickel-based catalysts with different promoter metals (Cu, Mg and Co) in the $CO_2$ reforming of HDPE were also studied. It was found that Ni-Co-Al had an excellent anti-coking performance, with no detectable formation of coke on the catalyst surface. Moreover, the syngas production was significantly improved by the addition of Co compared to the Cu and Mg metal promoters. The $CO_2$ conversion for Ni-Co-Al catalyst was also the highest at 57.62 %. Further investigation of the effect of Co concentration on $CO_2$ reforming of HDPE showed that the higher Co content, the higher syngas production and $CO_2$ conversion.

**Keywords:** Waste; Plastics; Reforming; Carbon dioxide; Catalyst

## 1. Introduction

Recently, many efforts have been made to reduce $CO_2$ emissions to the atmosphere because of the projected high environmental impact related to climate change. The major source of $CO_2$ emissions is from fossil fuelled energy systems and the mitigation strategies to reduce $CO_2$ include carbon capture. Such processes are likely to generate large quantities of $CO_2$ which opens opportunities for $CO_2$ utilisation. The reforming of methane with $CO_2$ (dry reforming) for the production of $H_2$ and CO rich syngas has been reported to be promising by some researchers [1-3]. In addition, waste plastics could be a potential source for the methane and other hydrocarbons required in the reforming process. Pyrolysis of waste plastics produces gaseous product which are rich in hydrocarbons. These hydrocarbons have the potential to be reformed with $CO_2$ to produce a $H_2$ and CO syngas.

It is known that the addition of catalysts in the reforming process has a beneficial influence on syngas production. The most widely used catalysts tend to be nickel-based and have been used to enhance steam reforming, partial oxidation, hydrogenation and dry reforming. Their high stability and catalytic activity, and lower cost compared to noble metal catalysts are the reasons that they are preferred for the reforming process [4,5]. However, nickel catalysts are known to be prone to deactivation due to coke formation on the catalyst and nickel sintering [6-8]. It has been suggested by many studies that adjusting the support, addition of active metals and suitable catalyst preparation methods could improve catalyst stability [9-12]. Lv, et al. investigated the pre-treatment of the silica supported nickel catalyst with ethylene glycol for the dry reforming of $CH_4$ [13]. They reported that the ethylene glycol pre-treatment modified the surface properties of the silica support, resulting in lower deposition of carbon on the catalyst and a lower degree of sintering. Different nickel catalysts supported on various supports (δ,θ-$Al_2O_3$, $MgAl_2O_4$, $SiO_2$-$Al_2O_3$ and $ZrO_2$-$Al_2O_3$) were also investigated by Damyanova, et al. for inhibition of carbon formation for dry reforming of $CH_4$ [14]. They found that there was a strong interaction between nickel oxide species and $MgAl_2O_4$ which retarded the sintering of the nickel and also reduced the formation of coke.

This paper is a continuation from our previous study [15] related to earlier work investigating the two-stage, pyrolysis-reforming of HDPE in relation to the steam and $CO_2$ reforming agent. The aim of this present paper is to study the effect of the addition of different metal promoters in the form of cobalt, magnesium and copper into nickel-alumina based catalysts in relation to the production of product syngas. Carbon dioxide conversion and carbon formation on the catalysts was also investigated. Further investigation into the relation of the different molar ratios of Ni-Co-Al on syngas quality has also been conducted.

## 2. Materials and Methods

### 2.1 Materials

The high density polyethylene (HDPE) feedstock was obtained as 2 mm waste polymer pellets from Regain Polymers Ltd, UK. From the elemental analysis, the composition of the waste HDPE was 82 wt.% of carbon and 18 wt.% of hydrogen.

Several Ni-based alumina catalysts, Ni-Al, Ni-Mg-Al, Ni-Cu-Al and Ni-Co-Al, were used in this study. Catalyst preparation was based on the rising-pH method [5]. $Mg(NO_3)_2.6H_2O$, $Cu(NO_3)_2.2.5H_2O$ or $Co(NO_3)_2.6H_2O$ was added to $Ni(NO_3)_26H_2O$

and $Al(NO_3)_39H_2O$ and dissolved in 200 ml deionised water with moderate stirring at 40 °C. 1 M ammonium solution, as the precipitant was then added to the aqueous solutions until the PH value of 8.3 was reached. The precipitate that was formed was filtered, dried (105 °C) and calcined (750 °C). The molar ratios for Ni-Al, Ni-Mg-Al and Ni-Cu-Al were 1:1, 1:1:1 and 1:1:1 respectively. In addition, to investigate the influence of Co concentration on the syngas production, Ni-Co-Al molar ratios of 1:0.5:1, 1:1:1 and 1:2:1 were also investigated. All the catalysts were crushed using a mortar and pestle and finally sieved using a 50-212 μm particle sieve.

## 2.2 Characterization of catalysts

A Nova 2200e surface area and pore analyser was used to obtain the Brunauer, Emmet and Teller (BET) surface area of each catalyst using the nitrogen adsorption technique. A Bruker D-8 diffractometer was used to record the X-ray diffraction (XRD) patterns of the prepared catalysts using a Cu-Kα radiation X-ray source with a Vantec position sensitive detector. The range was 10° - 70° with a scanning step of 0.05°. The pattern identification was obtained using HighScore Plus software.

Temperature programmed reduction ($H_2$-TPR) of the prepared catalysts used a Stanton-Redcroft thermogravimetric analyser (TGA). During the $H_2$-TPR analysis, each fresh catalyst (20 mg) was first heated from room temperature to 150 °C at 20 °C $min^{-1}$ and held for 30 min to remove water, then heated at 10 °C $min^{-1}$ to a final temperature of 900 °C. The feed gas used was hydrogen (5% $H_2$ balanced with $N_2$).

The carbon deposited on the used catalysts were characterised using scanning electron microscopy (SEM) (LEO 1530) and also temperature-programmed oxidation

(TPO) using a Shimadzu-50 thermogravimetric analyser (TGA). For TPO, the temperature programme was room temperature to 800 °C at 15 °C min$^{-1}$ heating rate.

## 2.3 Experimental system.

The pyrolysis-reforming experiments with HDPE involved a two-stage fixed bed reactor (Figure 1). The dimensions of the reactor were 250 mm x 30 mm i.d. heated by two separate electrical furnaces (1.2 kW each). The first stage consisted of pyrolysis of the HDPE and the product pyrolysis gases were transferred to the second stage where dry reforming of the hydrocarbons took place in the presence of $CO_2$ and the Ni-based catalyst. The experimental procedure involved 1 g of catalyst which was placed in the second stage catalytic reactor and was first heated to 800 °C. The first stage pyrolysis reactor which contained 2 g of waste HDPE was then heated up to 500 °C at 10 °C min$^{-1}$. Nitrogen was used as carrier gas. Carbon dioxide with a flow rate of 6.0 g h$^{-1}$ was injected into the second stage reforming furnace. The gaseous products after the two-stage, pyrolysis-reforming process were passed through a three stage dry-ice cooled condenser system to condense any liquids. The non-condensed gases were collected in a Tedlar$^{TM}$ gas sample bag for later, off-line gas analysis. Repeat experiments were performed to ensure consistency and accuracy of the results as well as the stability of the reactor.

The collected gases in the gas sample bag were analysed by a gas chromatography (GC). A Varian 3380 GC with a 80-100 mesh HayeSep column and $N_2$ carrier gas and flame ionisation detector was used to analyse hydrocarbons ($C_1$-$C_4$). Another Varian 3380 GC analysed $H_2$, CO, $O_2$ and $N_2$ on a 2 m long x 2 mm i.d., 60-80 mesh molecular sieve column with Ar carrier gas and thermal conductivity detector (TCD). On a separate column in the same Varian 3380 GC, $CO_2$ was analysed on a 2 m long x 2 mm i.d. HayeSep 80-100 mesh column with Ar carrier gas and TCD.

The conversion of carbon dioxide (as percentage) was calculated according to the following formula:

$$XCO_2 = \frac{[molsCO_2]in - [molsCO_2]out}{[molsCO_2]in} \times 100$$

## 3. Results and discussion

### 3.1 Fresh catalyst characterization.

Table 1 shows the surface area of the freshly prepared nickel based catalysts, Ni-Al, Ni-Cu-Al, Ni-Mg-Al and Ni-Co-Al and the three different cobalt containing catalyst compositions for the Ni-Co-Al catalyst. The surface area is generally related to the catalytic activity of the catalyst, in which high surface area typically improves the activity of the catalyst [16,17]. Addition of the Cu, Mg and Co promoters to the Ni-Al catalyst reduced the surface area of the catalysts. We also reported earlier a similar effect of the addition of Mg into a Ni-Al catalyst where catalyst surface area was reduced from 155 $m^2 g^{-1}$ (Ni-Al (1:2)) to 99 $m^2 g^{-1}$ (Ni-Mg-Al (1:1:1)) [18].

The XRD spectra patterns of the Ni-Al, Ni-Cu-Al, Ni-Mg-Al and Ni-Co-Al catalysts were obtained from the X-ray diffraction analysis and the results are shown in Figure 2. The metal appears to be well distributed throughout the catalysts. All of the catalysts exhibited XRD intensity peaks for the presence of NiO, $\gamma Al_2O_3$ and $NiAl_2O_4$. In addition, four intensity peaks representative of CuO were observed for the Ni-Cu-Al catalyst [16], two peaks for MgO and a peak of NiMgO for the Ni-Mg-

Al catalyst [19] and five peaks of $Co_3O_4$ for the Ni-Co-Al catalyst [20,21]. Since the catalyst was not be treated or reduced prior to the analysis, the XRD patterns show that all the metal added to the catalysts remains in their oxide forms as expected. The XRD patterns for the different ratios of Ni-Co-Al catalyst are shown in Figure 3. The patterns were similar, however small difference can be seen on the diffraction peaks, in which the peaks became more sharper as the amount of cobalt was increased, as the ratio was increased from 1:0.5:1 to 1:2:1.

Figure 4 shows the $H_2$-TPR profiles of the fresh catalysts. The main reduction peaks of both Ni-Al and Ni-Mg-Al catalyst occur at high temperature at around 750 °C to 850 °C, showing the strong interaction between the metal and the support. In contrast, the Ni-Cu-Al catalyst demonstrated a low intensity peak at a temperature between 230 °C and 260 °C, which may be attributed to reduction of NiO that was weakly interacted with the support material [9]. The Ni-Co-Al catalysts with increasing cobalt content exhibited similar profiles of two reduction peaks. The first peak was observed at a temperature between 290 – 450 °C and the second reduction peak was detected between 550 – 730 °C. The first peak may be assigned to the reduction of $Co_3O_4$ and NiO species which occur at the same time and the second peak suggests the reduction of $NiCo_2O_4$ and/or $Co_3O_4$; NiO species and metal aluminate spinel species (such as $NiAl_2O_4$ and $CoAl_2O_4$) having strong interaction with support. A Similar trend has been reported in studies of Ni-Co-Al catalysts with the addition of Sr [22]. The complete reduction of Ni-Co bimetallic catalysts was reported to involve two or more overlapping reduction peaks due to the simultaneous reduction of $Co_3O_4$ and NiO species [22].

## 3.2 Pyrolysis-catalytic $CO_2$ reforming of HDPE

### 3.2.1. Ni-Al catalyst:

The pyrolysis-catalytic $CO_2$ reforming of HDPE with the Ni-Al catalyst was carried out at a catalyst temperature of 800 °C. The non-catalytic pyrolysis-$CO_2$ reforming of HDPE was also carried out where sand was used as the substitute for catalyst. Experiments without any catalyst or sand were also carried out as a baseline experiment for comparison with the results when sand or catalyst was used. The product yields are shown in Table 2 and the gas compositions of the experimental results are presented in Figure 5. Figure 6 shows the carbon deposition and the $CO_2$ conversion from the pyrolysis-dry reforming of HDPE. The carbon deposition was the carbon deposited on the catalyst/sand after the experiment.

Table 2 shows that in the absence of catalyst and with no $CO_2$ reforming agent, the HDPE was pyrolysed to produce a liquid product (33.5 wt.%), gas (46.9 wt.%) and significant deposition of carbon on the sand surface. The pyrolysis residue from HDPE was negligible. The residue was measured by weighing the sample holder in the first stage reactor (Figure 1) before and after the experiment. Pyrolysis of HDPE usually produces high yields of oil/wax, typically ~80 wt.% [23]. However, in this work for the uncatalysed experiments, the pyrolysis gases pass through the sand bed at a temperature of 800 °C and are cracked to produce higher gas yield and significant deposits of carbon on the sand. The introduction of $CO_2$ in the non-catalytic experiment produced a marked increase in gas yield from 46.9 to 90.6 wt.%. It is suggested that the $CO_2$ was involved in the cracking and reforming of the hydrocarbon oil/wax to produce gases due to the marked reduction of liquid yield from 33.5 to 2.0 wt.%. $CO_2$ reforming also reduced the carbon deposited on the sand from 19.5 to 2.8 wt.%.

The introduction of the Ni-Al catalyst in the absence of $CO_2$ produced a slight decrease on the gas yield from 46.9 wt.% (sand) to 33.7 wt.%. This decrease in gas yield corresponded to a high carbon deposition of 56.0 wt.% on the Ni-Al catalyst and reduction of liquid yield to 7.5 wt.%. The introduction of $CO_2$ to the second reactor to produce dry $CO_2$ catalytic reforming reactions of the HDPE pyrolysis gases resulted in an improved production of gases to 93.2 wt.% while reducing the carbon deposited on the catalyst to 1.0 wt.%.

Figure 5 shows the analysis of the gases produced from the pyrolysis-catalytic $CO_2$ reforming of HDPE with the Ni-Al catalyst. Compared with the gas produced in the absence of catalyst (sand) and absence of $CO_2$, where high concentrations of $CH_4$ and $C_2$-$C_4$ were found, the introduction of $CO_2$ in the absence of the catalyst (sand) produced a syngas with increased concentrations of $H_2$ and CO. However, with the introduction of the Ni-Al catalyst to the $CO_2$ reforming process, the concentration of CO markedly increased, with also high concentrations of $H_2$. The syngas ($H_2$+CO) production was increased from 20.01 $mmol_{syngas}\ g^{-1}_{HDPE}$ for non-catalytic and no $CO_2$ experiment to 138.81 $mmol_{syngas}\ g^{-1}_{HDPE}$ for the $CO_2$ reforming of HDPE with the Ni-Al catalyst (Table 2). The increase of $H_2$ and CO concentration and the decrease of $CH_4$ and $C_2$-$C_4$ hydrocarbon in the gas yield in the $CO_2$ reforming of HDPE are due to the promotion of $CO_2$/dry reforming reactions (reaction 1) in the second reactor. This can be supported by the increase in $CO_2$ conversion from 40.81% for $CO_2$ reforming of HDPE with sand to 54.46% with the Ni-Al catalyst (Figure 6).

$$CnHm + nCO_2 = 2nCO + \frac{m}{2}H_2 \qquad \text{(Reaction 1)}$$

The used Ni-Al catalyst was analysed by TPO and SEM and the DTG-TPO thermograms and SEM micrographs are shown in Figure 7 and Figure 8 respectively.

The DTG-TPO thermograms of the reacted Ni-Al catalyst with and without $CO_2$ (Figure 7), indicated a mass increase in the DTG-TPO thermograms at around 450 °C which was attributed to the oxidation of the Ni particles during the oxidation process [24]. A large peak of carbonaceous coke oxidation occurred at a temperature of ~650 °C for the Ni-Al catalysts in the absence of $CO_2$. The oxidation peak at ~650 °C was assigned to the oxidation of graphitic filamentous carbons which are more resistant to oxidation compared to amorphous carbons which are typically oxidised at ~450 °C [25]. Figure 8 confirmed the presence of large quantities of filamentous carbons. In the presence of $CO_2$ and the Ni-Al catalyst there was only a small oxidation peak at 650 °C, suggesting low carbon deposition, also confirmed by the carbon deposition shown in Table 2 and the SEM micrograph in Figure 8. It is suggested that the reduction of carbon deposited on the catalyst might be due to the reaction between carbon and $CO_2$ (Reaction 2) [26]. Guczi, et al. [26] investigated the formation of surface carbon on a $Ni/MgAl_2O_4$ catalyst for the $CO_2$ reforming of methane. It was reported that the accumulation of carbon decreased at high temperature and most of the carbonaceous coke was removed by this reverse-Boudouard reaction.

$$C + CO_2 = CO \qquad \text{(Reaction 2)}$$

### 3.2.2 Ni-Cu-Al, Ni-Mg-Al and Ni-Co-Al catalysts

Cu, Mg and Co were added to the Ni-Al catalyst to investigate the influence of these metals towards higher syngas production, lower coke formation and higher $CO_2$

conversion compared to the Ni-Al catalyst. Table 2 and Figure 5 illustrate the effect of Cu, Mg or Co addition to the Ni-Al catalyst on syngas ($H_2$ and CO) production and gas composition.

In the experiments with no $CO_2$ addition to the second stage reactor, the gas yield for the Ni-Al catalyst was 33.7 wt.%, when Cu was added to the Ni-Al catalyst the gas yield increased to 52.3 wt.%, and for Mg addition and Co addition, the gas yield showed less of an increase to 39.9 wt.% and 38.6 wt.% respectively (Table 2). There was also a small decrease in the amount of carbon deposited on the catalyst when the metal promoter was added, decreasing from 56.0 wt.% for the Ni-Al catalyst to 43.5 wt.% for Cu addition, 43.0 wt.% for Mg addition and to 49.5 wt.% for Co addition Figure 5 shows the gas yields for the pyrolysis-catalysis of HDPE with Ni-Cu-Al, Ni-Mg-Al and Ni-Co-Al catalysts in the absence of $CO_2$. The Ni-Cu-Al catalyst showed the highest $CH_4$ and other hydrocarbons concentrations, resulting in higher gas yield but lower syngas production compared to the Mg and Co nickel based catalysts. The syngas productions for pyrolysis-catalysis of HDPE were similar for all the catalysts in the absence of $CO_2$ at ~50 $\text{mmol}_{\text{syngas}}\ \text{g}^{-1}{}_{\text{HDPE}}$ (Table 2).

When $CO_2$ was introduced into the pyrolysis-catalytic $CO_2$ reforming of HDPE process, the amount of gases produced showed a small increase in the presence of the Ni-Cu-Al, Ni-Mg-Al and Ni-Co-Al catalysts compared to the gas yield using Ni-Al with $CO_2$ (Table 2). In addition, the relationship between carbon deposition and $CO_2$ conversion are shown in Figure 6. The carbon deposited on the catalyst showed only a small influence of the addition of the Cu and Mg promoters where carbon deposition was increased from 1.0 wt.% (Ni-Al) to 1.1 wt.% with Cu addition and decreased to 0.7 wt.% with Mg addition. However, there was no coke formation detected on the Ni-Co-Al catalyst. This is also in agreement with the results from

DTG-TPO thermograms in Figure 7. The carbon deposition results are also reflected in the carbon conversion data with lower coke deposition producing higher $CO_2$ conversion (Figure 6). The carbons formed on the Ni-Al catalyst with the addition of Cu, Mg and Co were also observed from SEM morphology (Figure 8). The Ni-Cu-Al and Ni-Mg-Al catalysts showed evidence of the presence of filamentous carbons, but the Ni-Co-Al catalyst showed no filamentous carbons.

Figure 5 shows the gas yields for the pyrolysis-catalytic $CO_2$ reforming of HDPE with the Ni-Cu-Al, Ni-Mg-Al and Ni-Co-Al catalysts. The concentrations of gases, as shown in Figure 5, indicated that there is little influence of Cu, Mg or Co metal addition to the Ni-Al catalyst in the presence of $CO_2$. The CO yields were influenced by metal addition, with the highest CO concentration with Co addition and Cu addition, producing lower CO compared to the Ni-Al catalyst. High $CH_4$ and other hydrocarbon concentrations were found for Cu addition with lower CO concentrations.

Table 2 shows that the addition of carbon dioxide produces an increase in syngas production ($H_2$ + CO) from 105.41 $\text{mmol}_{\text{syngas}}\ \text{g}^{-1}_{\text{HDPE}}$ in the presence of sand, but with no catalyst to 138.81 $\text{mmol}_{\text{syngas}}\ \text{g}^{-1}_{\text{HDPE}}$ for the Ni-Al catalyst. The addition of the Cu metal promoter to the Ni-Al catalyst reduced syngas production to 130.56 $\text{mmol}_{\text{syngas}}\ \text{g}^{-1}_{\text{HDPE}}$. However, the addition of the Mg and Co metal promoters to the Ni-Al catalyst increased syngas production to 146.96 $\text{mmol}_{\text{syngas}}\ \text{g}^{-1}_{\text{HDPE}}$ for the Ni-Mg-Al catalyst and to 149.42 $\text{mmol}_{\text{syngas}}\ \text{g}^{-1}_{\text{HDPE}}$ for the Ni-Co-Al catalyst. The syngas ($H_2$ and CO) production for catalytic – $CO_2$ reforming of HDPE were therefore in the order: Ni-Co-Al > Ni-Mg-Al > Ni-Al > Ni-Cu-Al (Table 2, Figure 5).

The syngas ($H_2$ and CO) production for catalytic – $CO_2$ reforming of HDPE were therefore in the order: Ni-Co-Al > Ni-Mg-Al > Ni-Al > Ni-Cu-Al (Table 2, Figure 5).

For the Ni-Cu-Al catalyst, this is also reflected in the $H_2$-TPR data (Figure 4), where Cu had a very weak metal-support interaction, resulting in low catalytic activity and consequently, the lowest syngas production and highest carbon deposition. The $H_2$-TPR data for the Ni-Co-Al catalyst suggest the strongest metal-support interaction and with the highest syngas production and lowest carbon formation on the catalyst surface suggesting the highest catalytic activity.

The results suggest that the addition of Co into the Ni-Al catalyst increased the syngas production and $CO_2$ conversion for the $CO_2$ reforming of HDPE. The reduction of carbon deposited on the catalyst surface was also observed. Zhang et al. have also reported a high catalytic activity of a Ni-Co catalyst for the $CO_2$ reforming of methane which was attributed to a strong metal-support interaction [27]. Others have also highlighted the importance of strong metal-support interaction of Ni-Co catalysts to enhance catalytic activity and the low coke formation properties of Ni-Co catalysts [28-30]. Liu et al. have suggested that Cu on the catalyst surface has a very weak interaction with $CO_2$ compared to other metals based on their density functional theory studies of $CO_2$ adsorption and decomposition on Fe, Co, Ni and Cu surfaces [31].

### 3.3 Ni-Co-Al catalysts with different molar ratios.

The Ni-Co-Al catalyst produced the highest syngas ($H_2$ and CO) yield, a high $CO_2$ conversion and no detectable carbon formation on the catalyst from the $CO_2$ reforming of HDPE. Further work was therefore undertaken to determine the influence of Co metal content in the Ni-Al catalyst in terms of optimising the syngas production, with high $CO_2$ conversion and low coke formation. Ni-Co-Al catalysts with molar ratios of 1:0.5:1, 1:1:1 and 1:2:1 were prepared.

Table 3 shows the influence of Co content on the product yield and gas composition for the $CO_2$ reforming of HDPE. There was a marginal increase in liquid yield and gas yield with the increase of molar ratio from 1:0.5:1 to 1:2:1. There was 0.9 wt.% of deposited carbon on the Ni-Co-Al catalyst with low Co content while no carbon was detected on the Ni-Co-Al catalysts with molar ratios of 1:1:1 and 1:2:1. This result is in agreement with results from DTG-TPO analysis where an intense oxidation peak was found at 600 °C for the Ni-Co-Al catalyst with low Co content (Figure 9). The SEM morphology of the Ni-Co-Al catalyst shown in Figure 10 also suggests that carbons were observed on the Ni-Co-Al catalyst with molar ratio of 1:0.5:1 and the amount were reduced at higher Co contents. The effects of different Ni-Co [31, 32] content have been investigated before, but there are few studies involving Co addition to a nickel-based catalyst. Jose-Alonso et al. [30] studied several different compositions of Co or Ni alumina supported catalysts for the $CO_2$ reforming of methane. They reported that increased metal content enhanced the $CO_2$ conversion and very low carbon deposits were formed, albeit that they used low metal concentrations (<4 wt.%). Zhang et al. [32] also reported that lower Ni-Co content catalysts had lower carbon deposition, but higher Ni-Co content produced significant carbon deposition when the catalysts were used over extended periods (~250 h). For the work reported here, there was no carbon deposition at the higher Co content Ni-Co-Al catalyst. However, no extended, time-on-stream experiments were carried out.

The composition of the product gases obtained from the experiments showed that the syngas ($H_2$ and CO) yield increased with the increase in Ni-Co-Al molar ratio from 139.74 to 155.13 $\mathrm{mmol_{syngas}\ g^{-1}{}_{HDPE}}$ for the $CO_2$ reforming of HDPE. The $CO_2$

conversion also increased from 56.11 wt.% to 60.08 wt.%. The increase of syngas yield, $CO_2$ conversion and also the decrease of $CH_4$ and other hydrocarbon concentrations are most likely due to the $CO_2$/dry reforming reaction (Reaction 1), which was more favourable in the catalyst with high Co contents.

Tables 2 and 3 show the $H_2$:CO molar ratio of the gas produced from the $CO_2$ reforming of HDPE in relation to the different catalysts used. The $H_2$:CO ratio in the absence of catalyst was high, ranging from 14.208 for the Ni-Al catalyst to 9.521 for the Ni-Cu-Al catalyst. However, when $CO_2$ was introduced as the reforming agent, the $H_2$:CO ratio was reduced to around 0.5. There have been several reports which highlight the importance of the $H_2$:CO ratio in relation to the end use application of the product syngas [33-35]. For example, Song and Guo [34] describe the range of syntheses possible using syngas to produce, for example liquid fuels through Fischer Tropsch synthesis, high value chemicals (e.g. aldehydes and alcohols) through the hydroformylation reaction, production of methanol through catalytic reaction with syngas etc. The properties of the syngas, in particular the $H_2$:CO ratio, influence the potential end-use synthesis of the syngas, for example an ideal $H_2$:CO ratio for Fischer Tropsch is around 2.0, but for the hydroformylation reaction the optimum $H_2$:CO ratio is around 1.0 [34]. Here, we have reported production of a syngas with a $H_2$:CO ratio of <1.0 for the dry reforming of HDPE. However, we have recently reported [15] on the steam, $CO_2$ and combined steam/$CO_2$ reforming of high density polyethylene using the two-stage pyrolysis-reforming reactor used here. The results showed that the $H_2$ and CO concentrations in the product syngas were influenced by the relative input amounts of steam/$CO_2$ reforming agent. Depending on the ratio of steam/$CO_2$ input, the syngas $H_2$:CO ratio could be manipulated to produce values between 1 and 2. Therefore, process conditions of the two-stage pyrolysis-reforming of plastics could be manipulated to produce a range of desired $H_2$:CO ratios depending on the steam and $CO_2$ input.

## 4. Conclusions

The addition of catalyst to the $CO_2$ reforming of HDPE improved the production of synthesis gas ($H_2$ and CO). It is suggested that the catalytic $CO_2$/dry reforming has a significant effect on the reformation of high molecular weight hydrocarbons to $H_2$ and CO in the catalytic dry reforming process. Ni-Al catalyst with the addition of Co content had higher catalytic activity than Cu and Mg. No detectable carbon formation on the surface of Ni-Co-Al catalyst suggested that the Ni-Co-Al catalyst produced a very high resistance to catalyst deactivation. Adjusting the Co content of the catalyst facilitates high catalytic activity for reforming of HDPE with $CO_2$, in which higher Co content contributes towards higher $CO_2$ conversion and lower coke formation.

## Acknowledgements

The authors are grateful for the financial support of the Majlis Amanah Rakyat (MARA) Malaysia (PhD scholarship for Juniza MD Saad) and the University of Leeds.

## References

[1] A. Serrano-Lotina, L. Daza, Influence of the operating parameters over dry reforming of methane to syngas, International Journal of Hydrogen Energy 39 (2014) 4089-4094.

[2] A. Albarazi, P. Beaunier, P. Da Costa, Hydrogen and syngas production by methane dry reforming on SBA-15 supported nickel catalysts: On the effect of promotion by $Ce_{0.75}Zr_{0.25}O_2$ mixed oxide, International Journal of Hydrogen Energy, 38 (2013) 127-139.

[3] Y.J.O. Asencios, E.M. Assaf, Combination of dry reforming and partial oxidation of methane on NiO–MgO–$ZrO_2$ catalyst: Effect of nickel content, Fuel Processing Technology, 106 (2013) 247-252.

[4] K. Tomishige, K. Fujimoto, Ultra-stable Ni catalysts for methane reforming by carbon dioxide, Catalysis Surveys from Asia, 2 (1998) 3-15.

[5] L. Garcia, A. Benedicto, E. Romeo, M.L. Salvador, J. Arauzo, R. Bilbao, Hydrogen production by steam gasification of biomass using Ni-Al coprecipitated catalysts promoted with magnesium, Energy & Fuels 16 (2002) 1222-1230.

[6] M.C.J. Bradford, M.A. Vannice, Catalytic reforming of methane with carbon dioxide over nickel catalysts I. Catalyst characterization and activity, Applied Catalysis A: General, 142 (1996) 73-96.

[7] J.R. Rostrupnielsen, J.H.B. Hansen, $CO_2$-Reforming of Methane over Transition Metals, Journal of Catalysis, 144 (1993) 38-49.

[8] M.M. Barroso-Quiroga, A.E. Castro-Luna, Catalytic activity and effect of modifiers on Ni-based catalysts for the dry reforming of methane, International Journal of Hydrogen Energy, 35 (2010) 6052-6056.

[9] A.E. Galetti, M.F. Gomez, L.A. Arrúa, M.C. Abello, Ni catalysts supported on modified ZnAl2O4 for ethanol steam reforming, Applied Catalysis A: General, 380 (2010) 40-47.

[10] S.R. de Miguel, I.M.J. Vilella, S.P. Maina, D. San José-Alonso, M.C. Román-Martínez, M.J. Illán-Gómez, Influence of Pt addition to Ni catalysts on the catalytic performance for long term dry reforming of methane, Applied Catalysis A: General, 435–436 (2012) 10-18.

[11] X. Du, D. Zhang, R. Gao, L. Huang, L. Shi, J. Zhang, Design of modular catalysts derived from NiMgAl-LDH@m-$SiO_2$ with dual confinement effects for dry reforming of methane, Chemical Communications, 49 (2013) 6770-6772.

[12] A.E. Castro Luna, M.E. Iriarte, Carbon dioxide reforming of methane over a metal modified Ni-Al2O3 catalyst, Applied Catalysis A: General, 343 (2008) 10-15.

[13] X. Lv, J.-F. Chen, Y. Tan, Y. Zhang, A highly dispersed nickel supported catalyst for dry reforming of methane, Catalysis Communications, 20 (2012) 6-11.

[14] S. Damyanova, B. Pawelec, K. Arishtirova, J.L.G. Fierro, Ni-based catalysts for reforming of methane with CO2, International Journal of Hydrogen Energy, 37 (2012) 15966-15975.

[15] J.M. Saad, M.A. Nahil, P.T. Williams, Influence of process conditions on syngas production from the thermal processing of waste high density polyethylene, Journal of Analytical and Applied Pyrolysis, (2014). http://dx.doi.org/10.1016/j.jaap.2014.09.027

[16] C. Wang, B. Dou, H. Chen, Y. Song, Y. Xu, X. Du, L. Zhang, T. Luo, C. Tan, Renewable hydrogen production from steam reforming of glycerol by Ni–Cu–Al, Ni–Cu–Mg, Ni–Mg catalysts, International Journal of Hydrogen Energy, 38 (2013) 3562-3571.

[17] P. Kim, Y. Kim, T. Kang, I.K. Song, J. Yi, Preparation of nickel-mesoporous materials and their application to the hydrodechlorination of chlorinated organic compounds, Catalysis Surveys from Asia, 11 (2007) 49-58.

[18] C. Wu, P.T. Williams, Investigation of Ni-Al, Ni-Mg-Al and Ni-Cu-Al catalyst for hydrogen production from pyrolysis–gasification of polypropylene, Applied Catalysis B: Environmental, 90 (2009) 147-156.

[19] C. Wang, B. Dou, H. Chen, Y. Song, Y. Xu, X. Du, T. Luo, C. Tan, Hydrogen production from steam reforming of glycerol by Ni–Mg–Al based catalysts in a fixed-bed reactor, Chemical Engineering Journal, 220 (2013) 133-142.

[20] C.K. Cheng, S.Y. Foo, A.A. Adesina, H2-rich synthesis gas production over $Co/Al_2O_3$ catalyst via glycerol steam reforming, Catalysis Communications, 12 (2010) 292-298.

[21] A.H. Fakeeha, W.U. Khan, A.S. Al-Fatesh, A.E. Abasaeed, M.A. Naeem, Production of hydrogen and carbon nanofibers from methane over Ni–Co–Al catalysts, International Journal of Hydrogen Energy, 40 (2015) 1774-1781

[22] A. Al-Fatesh, Suppression of carbon formation in $CH_4$–$CO_2$ reforming by addition of Sr into bimetallic Ni–Co/$\gamma$-$Al_2O_3$ catalyst Journal of King Saud University - Engineering Sciences, 27 (2015) 101-107.

[23] P.T. Williams, E.A. Williams E. A., Interaction of plastics in mixed plastics pyrolysis'. Energy & Fuels 13 (1999) 188-196.

[24] J.M. Rynkowski, T. Paryjczak, M. Lenik, On the nature of oxidic nickel phases in NiO/$\gamma$-$Al_2O_3$ catalysts, Applied Catalysis A: General, 106 (1993) 73-82.

[25] C. Wu, P.T. Williams. Investigation of coke formation on Ni-Mg-Al catalyst for hydrogen production from the catalytic steam pyrolysis-gasification of polypropylene'. Applied Catalysis B-Environmental 96 (2010) 198-207.

[26] L. Guczi, G. Stefler, O. Geszti, I. Sajó, Z. Pászti, A. Tompos, Z. Schay, Methane dry reforming with $CO_2$: A study on surface carbon species, Applied Catalysis A: General, 375 (2010) 236-246.

[27] J. Zhang, H. Wang, A.K. Dalai, Development of stable bimetallic catalysts for carbon dioxide reforming of methane, Journal of Catalysis, 249 (2007) 300-310.

[28] J. Xu, W. Zhou, Z. Li, J. Wang, J. Ma, Biogas reforming for hydrogen production over nickel and cobalt bimetallic catalysts, International Journal of Hydrogen Energy, 34 (2009) 6646-6654.

[29] N. Rahemi, M. Haghighi, A.A. Babaluo, M.F. Jafari, S. Khorram, Non-thermal plasma assisted synthesis and physicochemical characterizations of Co and Cu doped $Ni/Al_2O_3$ nanocatalysts used for dry reforming of methane, International Journal of Hydrogen Energy, 38 (2013) 16048-16061.

[30] D. San José-Alonso, M.J. Illán-Gómez, M.C. Román-Martínez, Low metal content Co and Ni alumina supported catalysts for the $CO_2$ reforming of methane, International Journal of Hydrogen Energy, 38 (2013) 2230-2239.

[31] C. Liu, T.R. Cundari, A.K. Wilson, $CO_2$ Reduction on Transition Metal (Fe, Co, Ni, and Cu) Surfaces: In Comparison with Homogeneous Catalysis, The Journal of Physical Chemistry C, 116 (2012) 5681-5688.

[32] J. Zhang, H. Wang, A.K. Dalai, Effects of metal content on activity and stability of Ni-Co bimetallic catalysts for $CO_2$ reforming of $CH_4$, Applied Catalysis A: General, 339 (2008) 121-129.

[33] T.X.Z. Jiang, V.L. Kuznetsov, P.P. Edwards. Turning carbon dioxide into fuel. Philosophical Transactions of The Royal Society A, 368, (2010) 3343-3364.

[34] X. Song, Z. Guo. Technologies for direct production of flexible $H_2/CO$ synthesis gas. Energy Conversion and Management, 47 (2006) 560-569.

[35] Y. Cao, X. Gao, J. Jin, H. Zhou, M. Cohron, H. Zhao, H. Liu, W. Pan. Synthesis gas production with an adjustable $H_2/CO$ ratio through the coal gasification process: Effects of coal ranks and methane addition. Energy & Fuels 22 (2008) 1720-1730.

**Table 1.** BET surface area of the prepared catalysts.

| Catalyst | Molar ratio | BET surface area ($m^2$ $g^{-1}$) |
|---|---|---|
| Ni-Al | 1:1 | 133 |
| Ni-Cu-Al | 1:1:1 | 73 |
| Ni-Mg-Al | 1:1:1 | 66 |
| Ni-Co-Al | 1:1:1 | 48 |
| Ni-Co-Al | 1:0.5:1 | 81 |
| Ni-Co-Al | 1:2:1 | 31 |

**Table 2.** Pyrolysis-dry reforming of HDPE with different catalysts.

| Catalyst<br>$CO_2$ flow rate (g $h^{-1}$) | None<br>0 | None<br>6.0 | Sand<br>0 | Sand<br>6.0 | Ni-Al<br>0 | Ni-Al<br>6.0 | Ni-Cu-Al<br>0 | Ni-Cu-Al<br>6.0 | Ni-Mg-Al<br>0 | Ni-Mg-Al<br>6.0 | Ni-Co-Al<br>0 | Ni-Co-Al<br>6.0 |
|---|---|---|---|---|---|---|---|---|---|---|---|---|
| Product yield (wt. %) | | | | | | | | | | | | |
| Gas | 38.1 | 93.9 | 46.9 | 90.6 | 33.7 | 93.2 | 52.3 | 96.2 | 39.9 | 97.6 | 38.6 | 94.8 |
| Liquid | 27.0 | 1.4 | 33.5 | 2.0 | 7.5 | 1.2 | 4.0 | 2.5 | 7.5 | 1.1 | 6.5 | 2.4 |
| Residue | 0.0 | 0.3 | 0.0 | 0.2 | 1.0 | 0.1 | 0.0 | 0.1 | 1.0 | 0.1 | 0.0 | 0.0 |
| Carbon deposition | 28.0 | 3.4 | 19.5 | 2.8 | 56.0 | 1.0 | 43.5 | 1.1 | 43.0 | 0.7 | 49.5 | 0.0 |
| Mass balance | 93.0 | 99.0 | 99.9 | 95.6 | 98.2 | 95.5 | 99.8 | 99.9 | 91.4 | 99.5 | 94.5 | 97.2 |
| Syngas yield<br>(mmol$_{syngas}$ g$^{-1}$$_{HDPE}$) | | | | | | | | | | | | |
| $H_2$ + CO production | 25.32 | 112.35 | 20.01 | 105.41 | 51.90 | 138.81 | 47.53 | 130.56 | 48.78 | 146.96 | 50.83 | 149.42 |
| $H_2$:CO molar ratio | - | 0.49 | - | 0.48 | 14.21 | 0.47 | 9.52 | 0.51 | 10.11 | 0.49 | 11.15 | 0.47 |

**Table 3.** Pyrolysis-dry reforming of HDPE with different molar ratios of Ni-Co-Al catalyst

| Catalyst<br>Ratio | Ni-Co-Al<br>(1:0.5:1) | Ni-Co-Al<br>(1:1:1) | Ni-Co-Al<br>(1:2:1) |
|---|---|---|---|
| Product yield (wt. %) | | | |
| Gas | 91.3 | 94.8 | 95.0 |
| Liquid | 2.1 | 2.4 | 2.9 |
| Residue | 0.1 | 0.0 | 0.0 |
| Carbon deposition | 0.9 | 0.0 | 0.0 |
| Mass balance | 94.4 | 97.2 | 97.9 |
| | | | |
| Gas composition ($g_{gas}$ $g^{-1}$ $_{HDPE}$) | | | |
| $H_2$ | 0.094 | 0.096 | 0.099 |
| CO | 2.615 | 2.852 | 2.965 |
| $CH_4$ | 0.087 | 0.086 | 0.079 |
| $C_2$-$C_4$ | 0.016 | 0.012 | 0.010 |
| | | | |
| $H_2$ + CO production ($mmol_{syngas}$ $g^{-1}_{HDPE}$) | 139.74 | 149.42 | 155.13 |
| $CO_2$ conversion (%) | 56.11 | 57.62 | 60.08 |
| $H_2$:$CO_2$ molar ratio | 0.50 | 0.47 | 0.47 |

## Figure Captions

**Fig. 1.** Schematic diagram of two-stage fixed bed, batch reactor.

**Fig. 2.** XRD spectra of the fresh catalysts: (a) Ni-Al (1:1) catalyst; (b) Ni-Cu-Al (1:1:1)catalyst; (c) Ni-Mg-Al (1:1:1) catalyst; (d) Ni-Co-Al (1:1:1) catalyst.

**Fig. 3.** XRD spectra of the different ratio of fresh Ni-Co-Al catalysts: (a) 1:0.5:1; (b) 1:1:1; (c) 1:2:1.

**Fig. 4.** Temperature programmed reduction ($H_2$-TPR) of the fresh catalysts: (a) Ni-Al (1:1) catalysts; (b) Ni-Cu-Al (1:1:1) catalyst; (c) Ni-Mg-Al (1:1:1)catalyst; (d) Ni-Co-Al (1:1:1) catalyst; (e) Ni-Co-Al (1:0.5:1) catalyst; (f) Ni-Co-Al (1:2:1) catalyst.

**Fig. 5.** Gas compositions for the pyrolysis-dry reforming of HDPE with different type of catalysts at a catalyst temperature of 800 °C.

**Fig. 6.** Relationship between carbon deposition and $CO_2$ conversion derived from pyrolysis-dry reforming of HDPE with different catalysts.

**Fig. 7.** DTG-TPO thermogram of different type of coked catalysts after pyrolysis-dry reforming of HDPE.

**Fig. 8.** SEM results of different type of coked catalysts calcined at 750 °C.

**Fig. 9.** DTG-TPO thermogram of the different ratio of Ni-Co-Al coked catalysts after pyrolysis-dry reforming of HDPE.

**Fig. 10.** SEM results of the different ratio of Ni-Co-Al coked catalysts calcined at 750 °C.

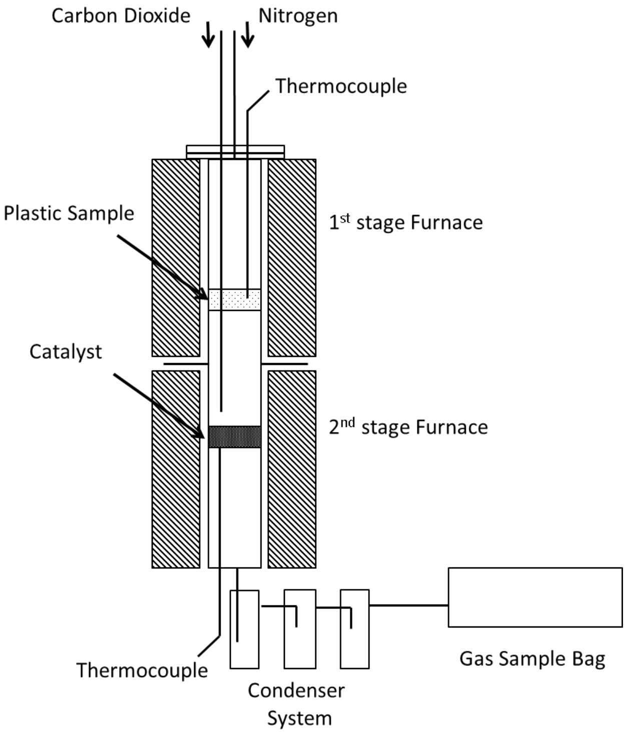
Carbon Dioxide
Nitrogen
Thermocouple
Plastic Sample
1st stage Furnace
Catalyst
2nd stage Furnace
Gas Sample Bag
Thermocouple
Condenser System

**Figure 1**

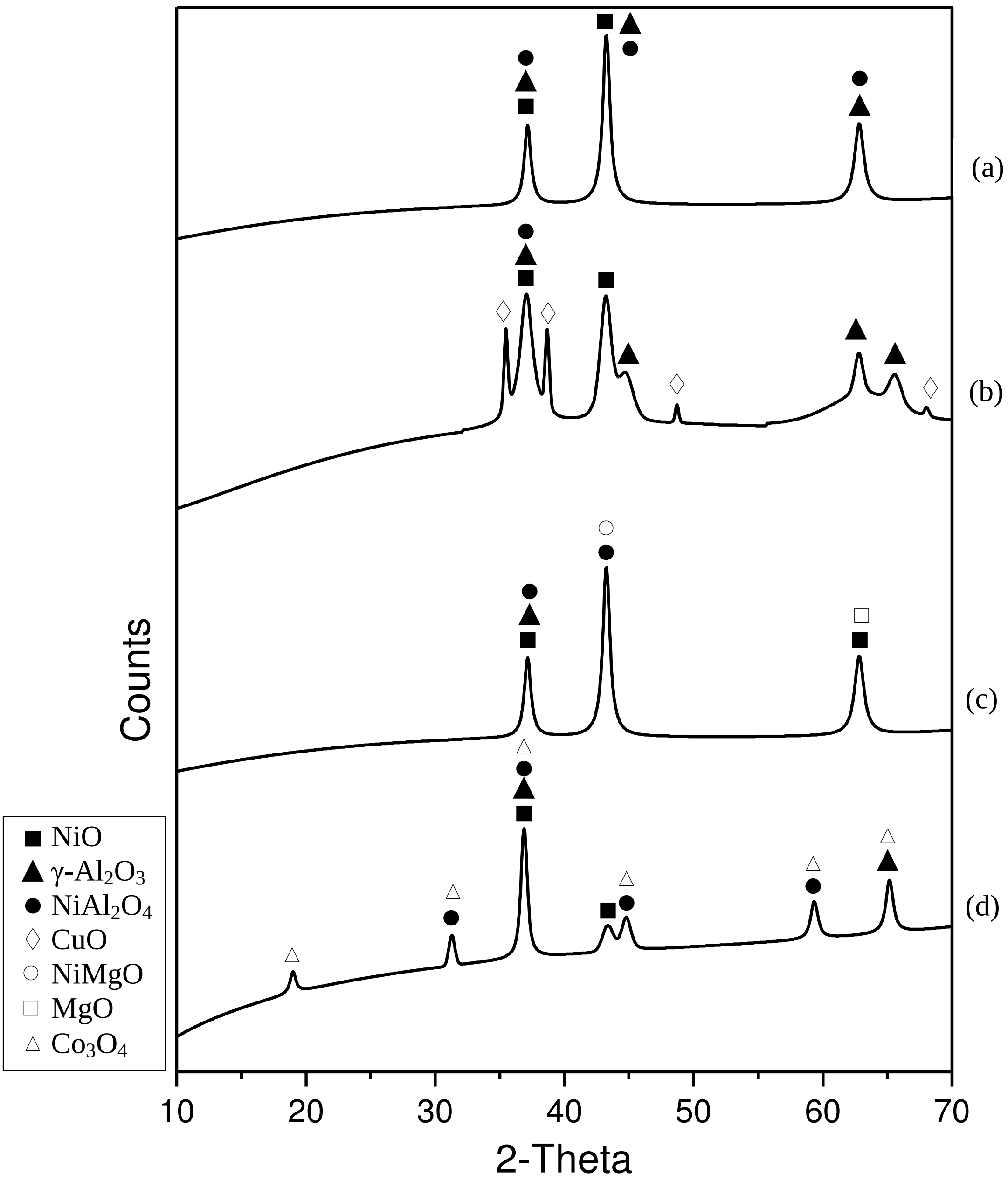
■ NiO
▲ γ-$Al_2O_3$
● $NiAl_2O_4$
◊ CuO
○ NiMgO
□ MgO
△ $Co_3O_4$
(a)
(b)
(c)
(d)
Counts
10
20
30
40
50
60
70
2-Theta

Figure 2

(b)

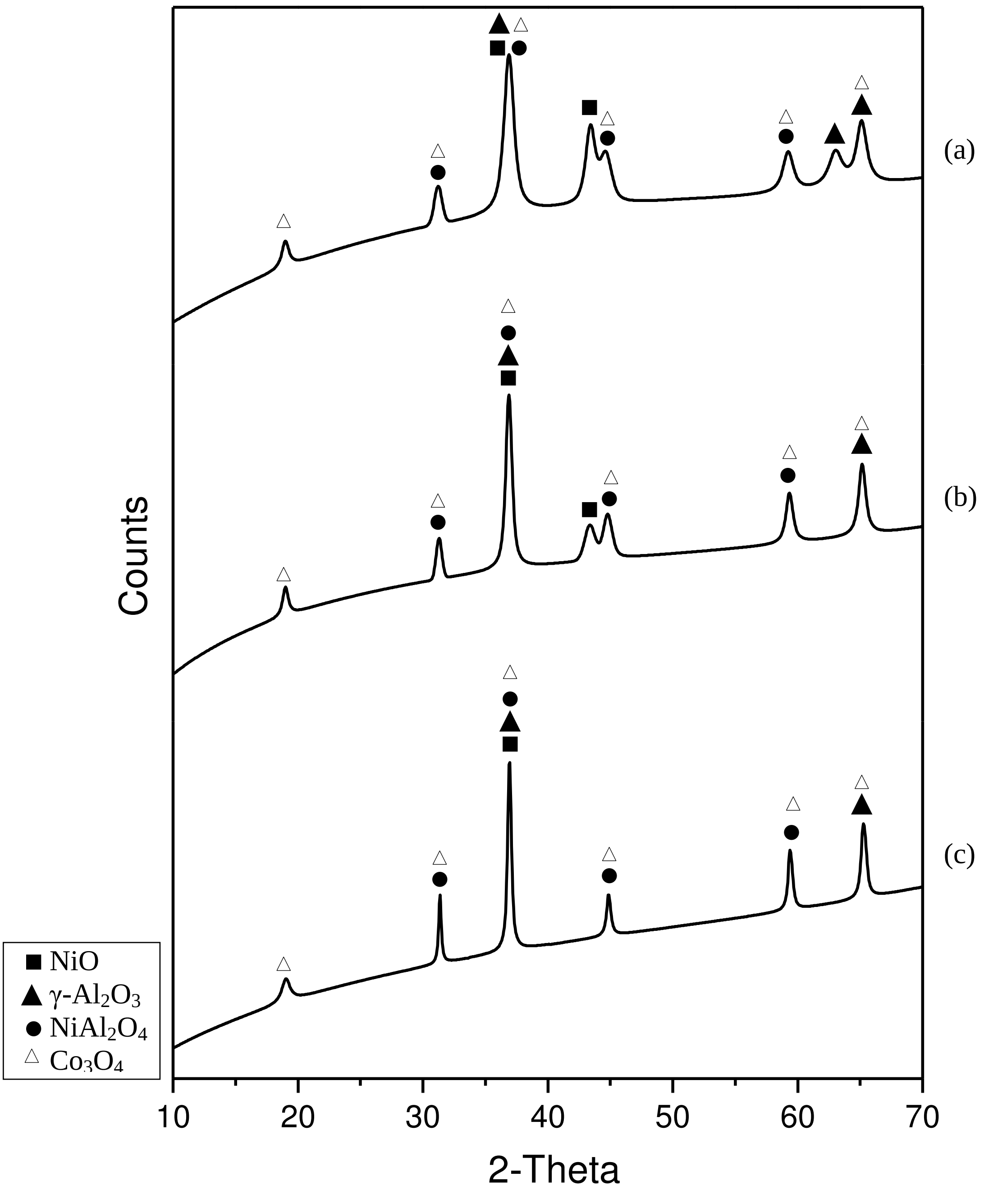

Counts
2-Theta
10
20
30
40
50
60
70
(a)
(b)
(c)
■ NiO
▲ γ-Al2O3
● NiAl2O4
△ Co3O4

**Figure 3**

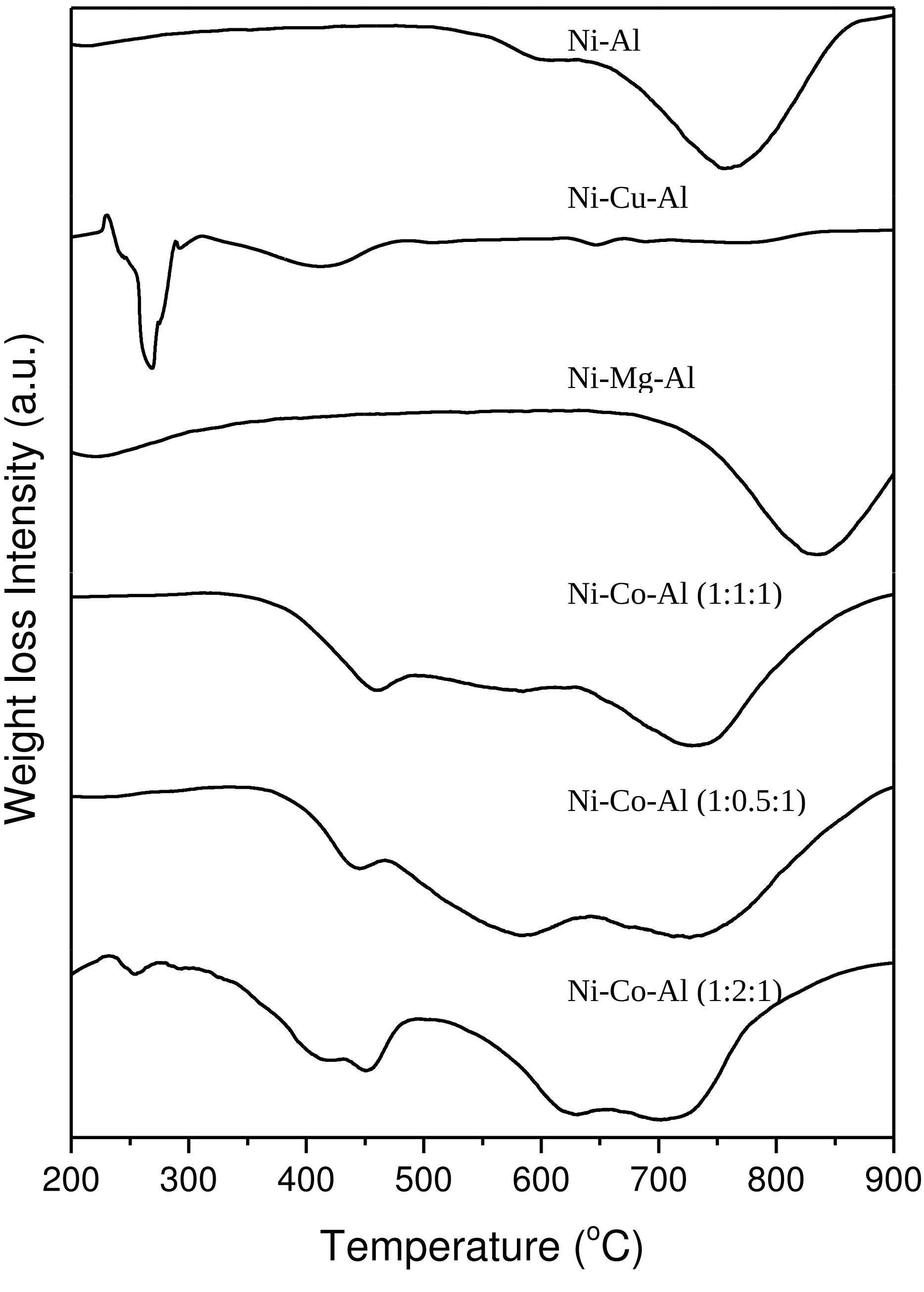
Ni-Al
Ni-Cu-Al
Ni-Mg-Al
Ni-Co-Al (1:1:1)
Ni-Co-Al (1:0.5:1)
Ni-Co-Al (1:2:1)
Weight loss Intensity (a.u.)
200
300
400
500
600
700
800
900
Temperature (°C)

**Figure 4**

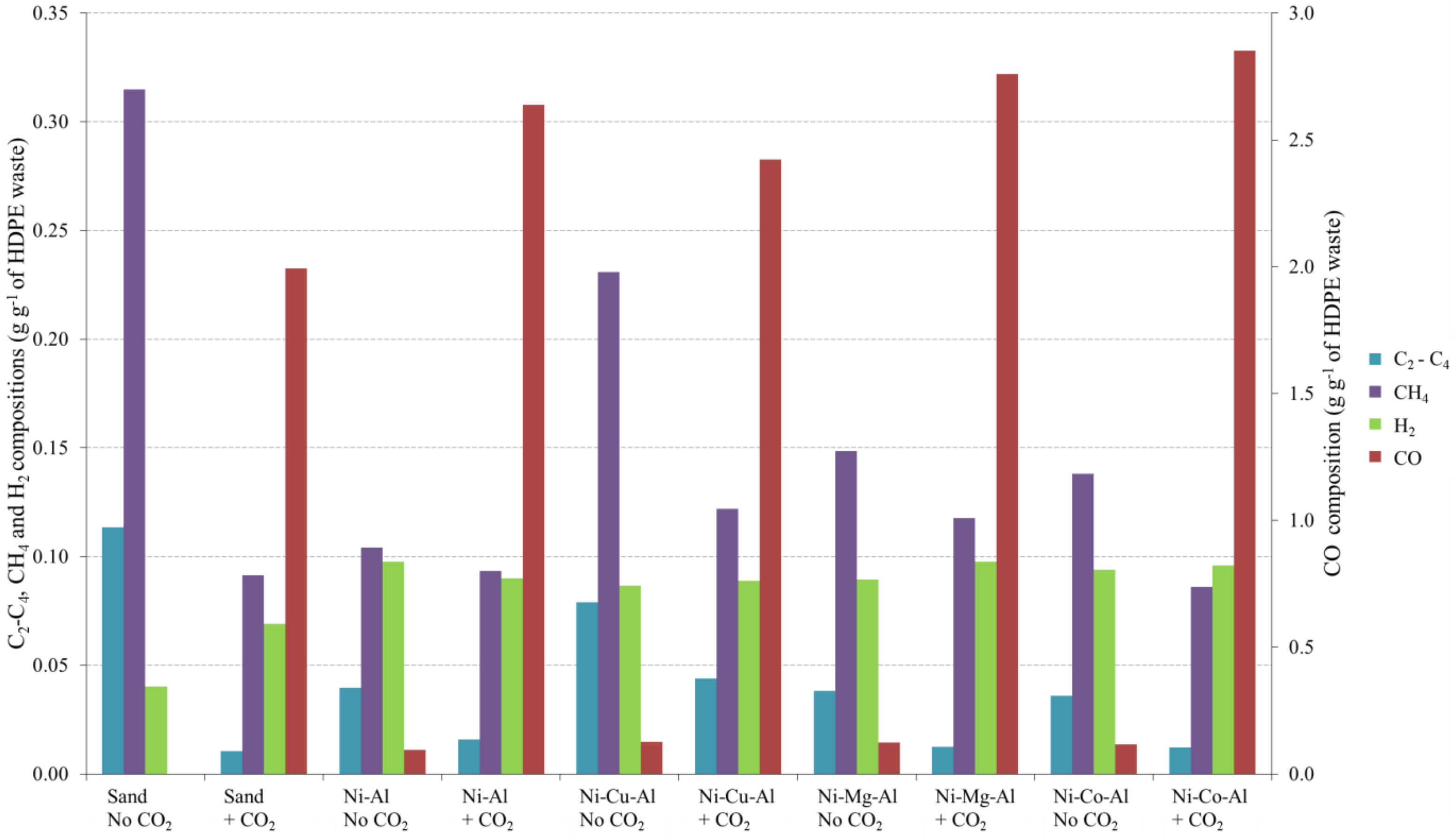
0.35
0.30
0.25
0.20
0.15
0.10
0.05
0.00
C2-C4, CH4 and H2 compositions (g g-1 of HDPE waste)
3.0
2.5
2.0
1.5
1.0
0.5
0.0
CO composition (g g-1 of HDPE waste)
Sand No CO2
Sand + CO2
Ni-Al No CO2
Ni-Al + CO2
Ni-Cu-Al No CO2
Ni-Cu-Al + CO2
Ni-Mg-Al No CO2
Ni-Mg-Al + CO2
Ni-Co-Al No CO2
Ni-Co-Al + CO2
C2 - C4
CH4
H2
CO

**Figure 5**

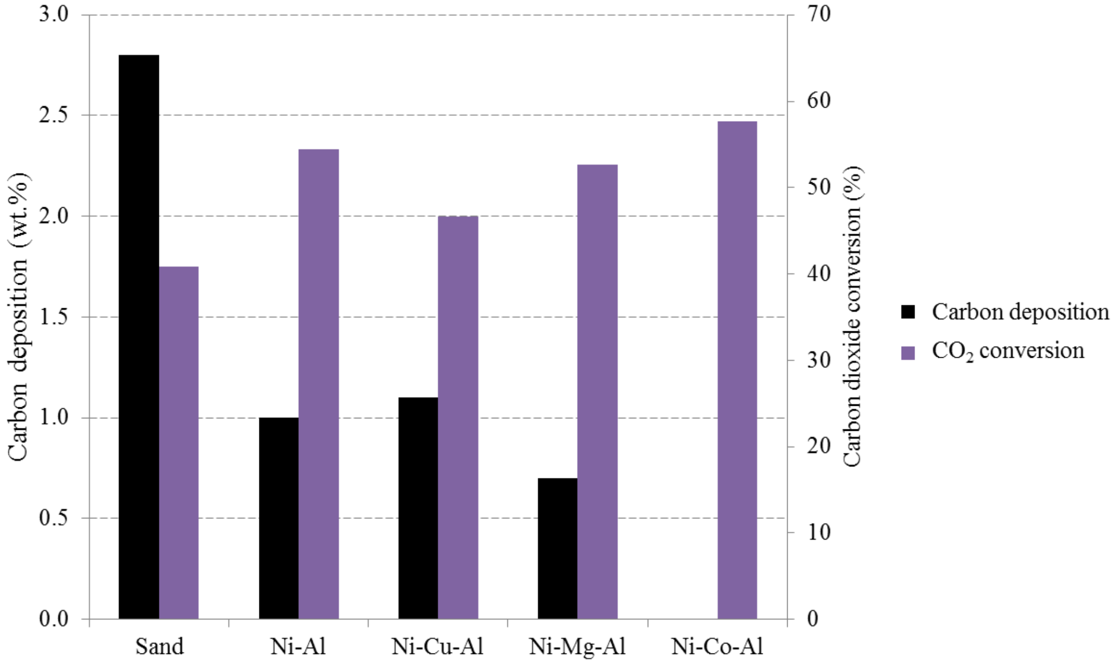
3.0
2.5
2.0
1.5
1.0
0.5
0.0
Carbon deposition (wt.%)
70
60
50
40
30
20
10
0
Carbon dioxide conversion (%)
Sand
Ni-Al
Ni-Cu-Al
Ni-Mg-Al
Ni-Co-Al
Carbon deposition
$CO_2$ conversion

**Figure 6**

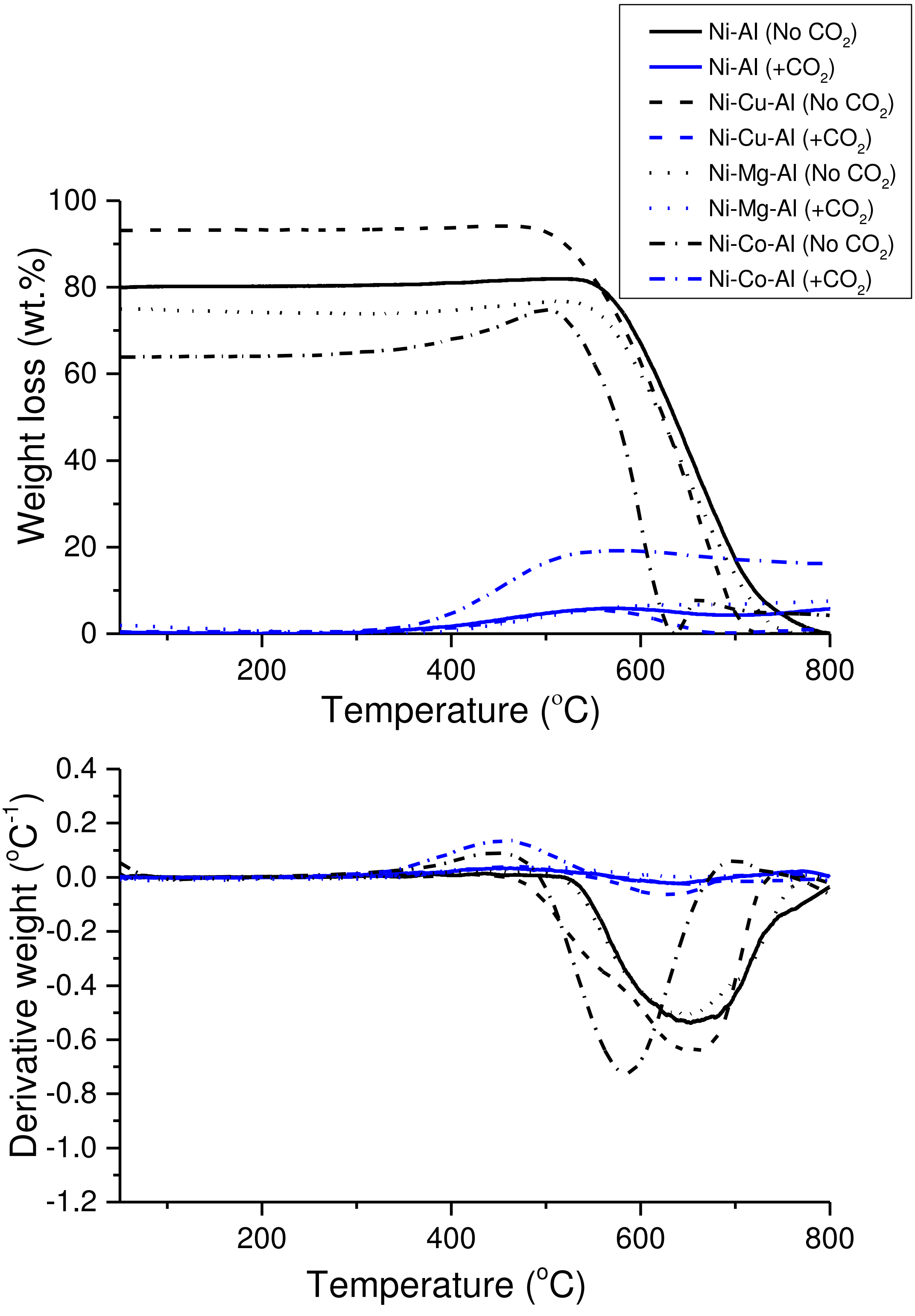
Ni-Al (No CO2)
Ni-Al (+CO2)
Ni-Cu-Al (No CO2)
Ni-Cu-Al (+CO2)
Ni-Mg-Al (No CO2)
Ni-Mg-Al (+CO2)
Ni-Co-Al (No CO2)
Ni-Co-Al (+CO2)
Weight loss (wt.%)
100
80
60
40
20
0
200
400
600
800
Temperature (°C)
Derivative weight (°C-1)
0.4
0.2
0.0
-0.2
-0.4
-0.6
-0.8
-1.0
-1.2
200
400
600
800
Temperature (°C)

**Figure 7**

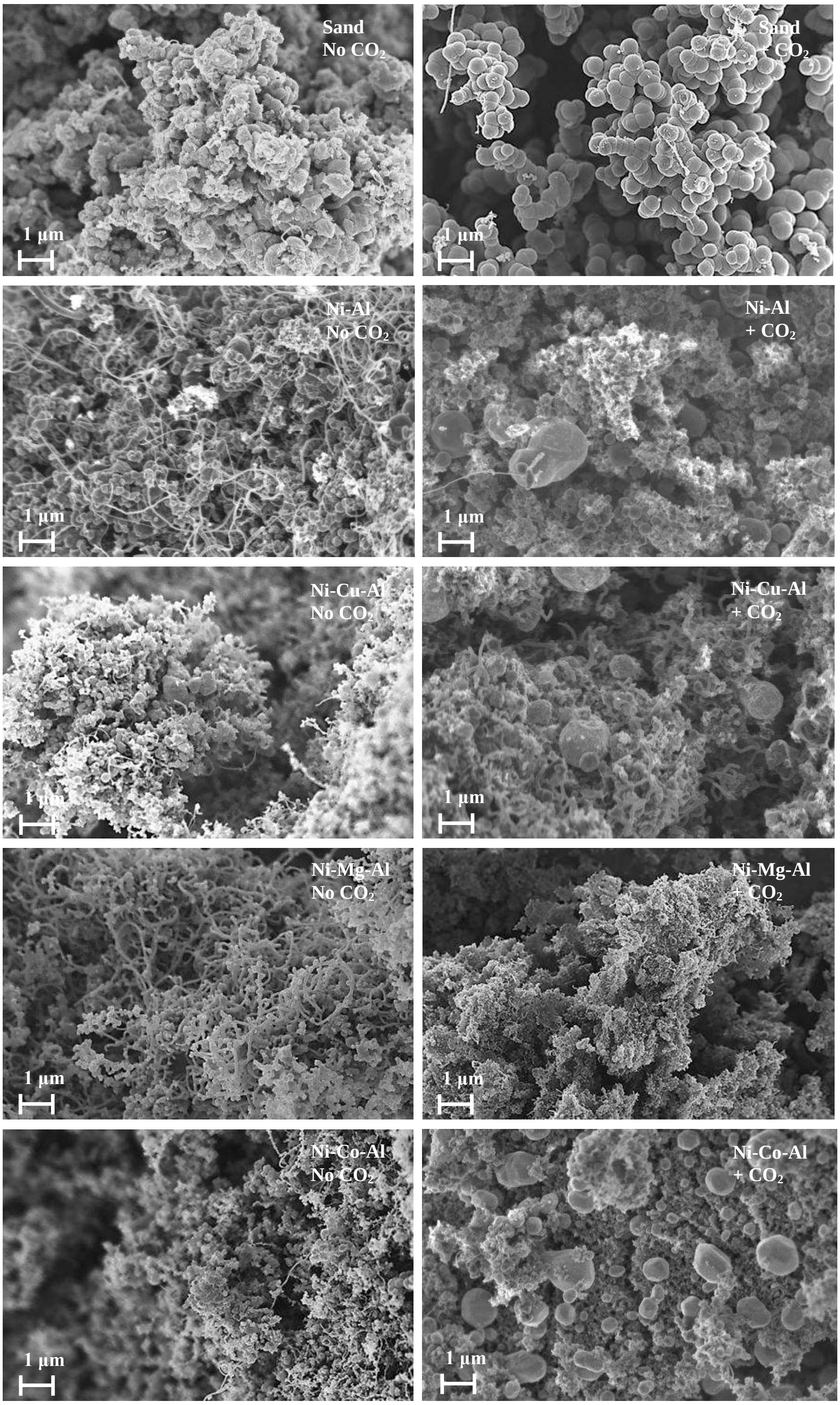
Sand
No CO$_2$
1 µm
Sand
+ CO$_2$
1 µm
Ni-Al
No CO$_2$
1 µm
Ni-Al
+ CO$_2$
1 µm
Ni-Cu-Al
No CO$_2$
1 µm
Ni-Cu-Al
+ CO$_2$
1 µm
Ni-Mg-Al
No CO$_2$
1 µm
Ni-Mg-Al
+ CO$_2$
1 µm
Ni-Co-Al
No CO$_2$
1 µm
Ni-Co-Al
+ CO$_2$
1 µm

**Figure 8**

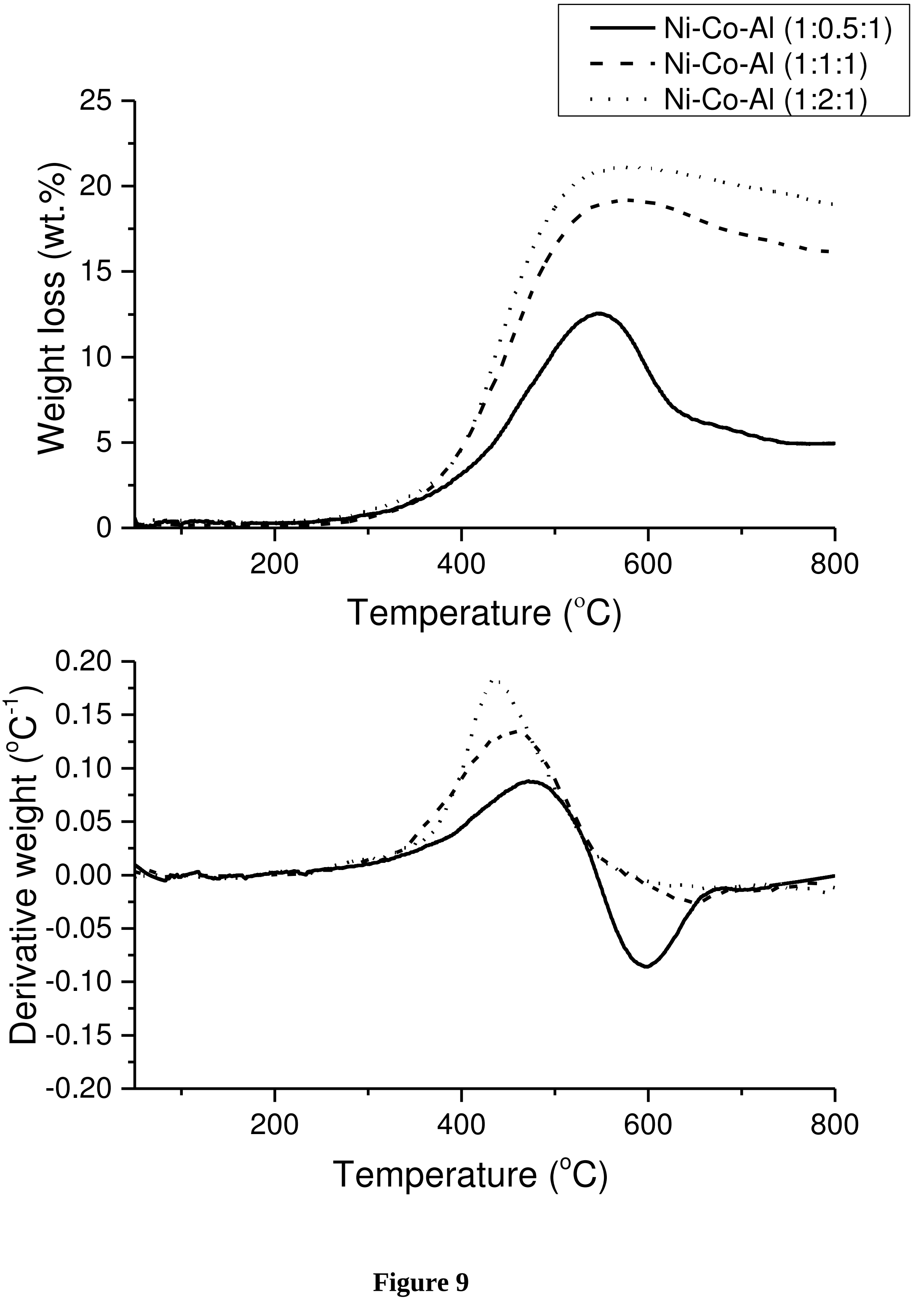
Ni-Co-Al (1:0.5:1)
Ni-Co-Al (1:1:1)
Ni-Co-Al (1:2:1)
Weight loss (wt.%)
25
20
15
10
5
0
200
400
600
800
Temperature (°C)
Derivative weight (°C⁻¹)
0.20
0.15
0.10
0.05
0.00
-0.05
-0.10
-0.15
-0.20
200
400
600
800
Temperature (°C)

**Figure 9**

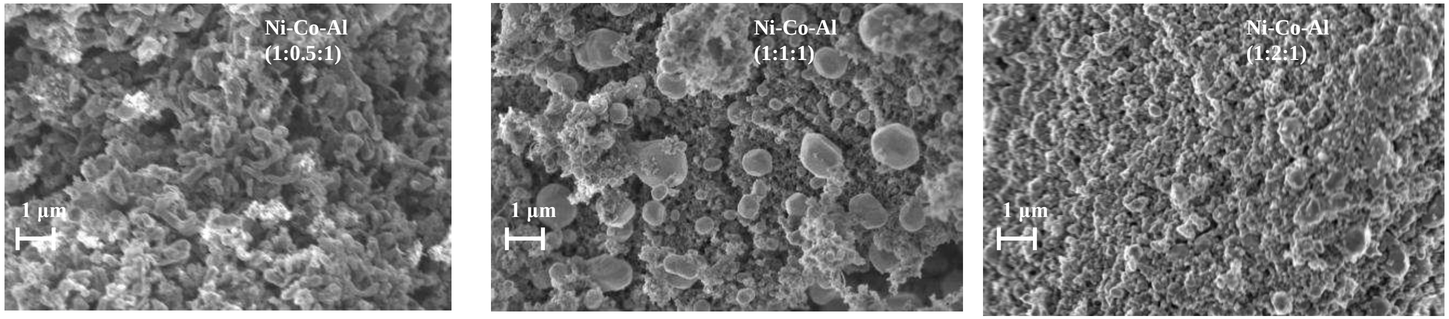

**Figure 10**